Propagation of terahertz radiation through random structures: An alternative theoretical approach and experimental validation

J. R. Fletcher, G. P. Swift,[a] De Chang Dai, J. A. Levitt, and J. M. Chamberlain
Department of Physics, University of Durham, Durham DH1 3LE, United Kingdom

(Received 6 June 2006; accepted 20 October 2006; published online 2 January 2007)

A model describing the propagation of terahertz frequency radiation through inhomogeneous materials is proposed. In such materials (e.g., powders or clothing), the size of the scattering centers, their separation, and the wavelength of the radiation are all commensurate. A phase distribution function is used to model the optical properties of a randomly structured transmitting layer. The predictions of the model are compared with exact (Mie) theory for isolated spherical scatterers and with previously published experimental data. Measurements of the transmission of terahertz radiation through a variety of samples in order to validate the present model are also reported. These include arrays of cylinders, textiles, powders, and glass balls. Overall, satisfactory agreement between the experimental data and theoretical predictions is obtained. © *2007 American Institute of Physics*. [DOI: 10.1063/1.2403860]

I. INTRODUCTION

Terahertz frequency sensing and imaging systems have many potential applications in a wide range of areas such as medicine, security and surveillance, process control. Although significant efforts have been expended on the development of imaging systems,[1] somewhat less attention has been paid to the issue of propagation through, or scattering from, realistic target materials which might be investigated with such systems. In practice, understanding the interaction of terahertz radiation with a wide range of irregularly structured materials is an essential part of the design of systems for terahertz sensing and imaging. On the one hand, scattering has adverse effects: it may produce false signatures in spectra when interference takes place within a scattering structure (e.g., fibers in clothing or granules of powder) or diminish and alter the return signal from a suspect item secreted below garments. On the other hand, it might be used to advantage to determine the characteristic size, texture, and location of an object concealed within a matrix of other material. Scattering effects are particularly relevant in this spectral regime, where the wavelength, and the size and separation of scattering centers are often commensurable.

Mittleman[2,3] has extensively studied the propagation of few-cycle pulses of terahertz radiation through a variety of inhomogeneous media, chiefly assemblies of Teflon spheres of various sizes. Diffuse scattering phenomena have also been investigated, and terahertz spectroscopy in the time domain has been used to identify specific scattering centers within a medium. It is noted from this work that there are considerable disagreements between experiment and the predictions of theory (e.g., Mie theory and the quasicrystalline approximation[2]) for the mean free path (MFP) as a function of wavelength for propagation through a random array of spherical scatterers. Mujumdar *et al.*[4] have also remarked that a classical effective medium approximation is of limited value in experimental and numerical studies of propagation through an assembly of subwavelength alumina spheres.

The purpose of this article is to provide a useful theoretical framework, validated by experiment, to predict the attenuation of terahertz radiation as it passes through inhomogeneous media such as textiles and powders. In due course, the present theory will be extended to predict the angular scattering properties of such media. A description of the organization of this article now follows. In Sec. II an approximation, the phase distribution model (PDM), is outlined which describes the overall transmission properties of a random system in terms of phase changes imposed on a wave front by the scattering centers. The experimental arrangements together with samples (textiles, absorbing, and nonabsorbing powders, and cylindrical arrays or phantoms) used for validation measurements are then outlined. A comparison of the predictions of the theory with exact (Mie) theory is then given for spheres and cylinders. There then follow sections in which the theory predictions for phantoms, textiles, and spherical grained powders are compared with experiment. A conclusion is then given. Further discussion of the phase distribution function is confined to the Appendix.

II. PHASE DISTRIBUTION MODEL

The theory of wave propagation through random media has a long history of development. Exact calculations based on Maxwell's equations are prohibitively difficult, and more convenient approximations are needed. For media in which the refractive index variations are not too large, a useful approach has been to regard the medium as equivalent to a succession of phase-changing layers perpendicular to the propagation direction and to neglect reflections. The use of this method to describe the effects of the ionosphere on radio waves was reviewed by Ratcliffe[5] and a theoretical analysis given by Fejer.[6] Further developments are described by Ishimaru.[7]

In the present work we extend this approach by introducing the concept of a phase distribution function to summarize

[a]Electronic mail: g.p.swift@durham.ac.uk

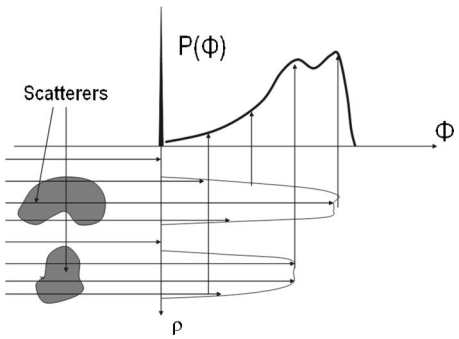

FIG. 1. Projection approximation for phase distribution P.

the relevant optical properties of a randomly structured transmitting layer and show how the bulk transmission is related to this distribution. The use of a distribution function leads naturally to the application of statistical methods. The transmitted wave emerging from the second face of a layer is completely determined by the amplitude and phase (and polarization) of the field across the surface. In general, this is a very detailed function of the transverse coordinates, but the relevant information for the calculation of forward transmission can be summarized in the distribution, $P(\varphi)$, defined below.

The thickness, d, of the layers into which the medium is divided in the theoretical model needs to satisfy two conditions:

Condition 1. The thickness should be large enough that correlations of scatterer positions between adjacent layers can be neglected. Waves that are multiply scattered in successive layers will not then contribute coherently to the forward propagation. The thickness should not be less than the correlation length for the scatterer density.

Condition 2. The layer should be sufficiently thin that simple approximation methods can be used to calculate the phase distribution. The range of validity of the projection approximation below is discussed in Ishimaru.[7]

For clothing fabrics, the medium can be modeled as a single layer for the calculation of the phase distribution. In the case of powders of randomly shaped grains, there is no long range correlation, and the layer thickness can be taken as a few times the grain size.

The phase change, φ, in a scalar wave propagating through a single layer is calculated by the projection approximation,[7]

$$\varphi(\rho) = 2\pi(n-1)t(\rho)/\lambda, \tag{1}$$

where $(n-1)$ is the refractive index difference between the scatterers and their surroundings, and $t(\rho)$ is the thickness of the scatterers within the layer, projected along the propagation direction at position ρ. The phase distribution function, $P(\varphi)$, illustrated in Fig. 1, gives the fraction of the wave front area having phase change φ, weighted by the amplitude of the wave, so that the fractional transmitted amplitude of the unscattered forward wave is given by

$$F = \int P(\varphi) e^{i\varphi} d\varphi. \tag{2}$$

The corresponding transmitted intensity, $|F|^2$, is the analog of the Strehl intensity[8] used in optical system design.

A. Absorbing scatterers

Absorbing scatterers with dielectric loss have a complex refractive index $(n+i\kappa)$, and projection of phase change along the propagation direction must allow for attenuation within the scatterer. The amplitude is reduced to

$$A(\rho) = \exp\left[\frac{-\kappa\varphi(\rho)}{n-1}\right], \tag{3}$$

with $\varphi(\rho)$ from Eq. (1). For a circular scatterer with radius a, the phase distribution is then

$$P_{SC}(\varphi) = \frac{-d(r^2/a^2)}{d\varphi} \exp\left(-\frac{\kappa\varphi}{n-1}\right). \tag{4}$$

The distribution is not normalized when there is energy loss by absorption. The transmitted amplitude can then be put into the form

$$F = \int P_S(\varphi) \exp\left[\varphi\left(i - \frac{\kappa}{n-1}\right)\right] d\varphi, \tag{5}$$

where P_S is the distribution for the same shape of scatterers without dielectric loss.

B. Attenuation

For any layer containing scatterers, the distribution, P, is restricted to the range from $\varphi=0$, originating in open gaps, to the maximum phase change, φ_M, produced by any region of the layer completely filled

$$\varphi_M = 2\pi d(n-1)/\lambda. \tag{6}$$

If the mean free path of the directly propagated beam is L, the transmitted intensity through a layer is given by

$$|F|^2 = \exp(-d/L), \tag{7}$$

and hence L can be found from the phase distribution function P using Eqs. (2) and (5).

For woven fabrics such as shirts and jackets, the warp and weft yarns are orthogonal and the phase changes they produce are dependent upon orthogonal coordinates. The phase distribution can then be calculated for each set of yarns separately, and the resulting transmission will be the product of transmissions through warp and weft separately. This reduces the problem from a three-dimensional model to two separate two-dimensional calculations, with consequent reduction in computational complexity.

The individual fibers constituting the yarn are generally too fine to be resolved at terahertz frequencies, and the yarn can be modeled as a uniform cylinder with an effective refractive index. There is very little information available on the terahertz properties of fibers used for clothing fabrics.[9] In the present work, the effective yarn index is treated as an

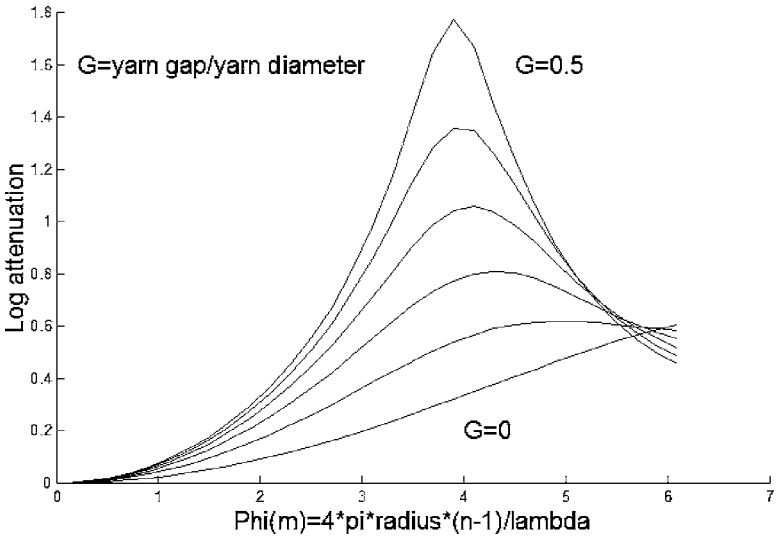

FIG. 2. Effects of yarn gap on attenuation.

empirical parameter with values in the range of 1.1–1.5. There is no evidence of dielectric loss at these frequencies.

It is found that the predicted transmission through a layer of warp or weft is strongly influenced by the ratio of the yarn diameter to the gap width between yarns. The phase difference between waves transmitted through the yarn and those through the gaps is proportional to frequency and, if the gaps are not small, this can result in destructive interference. Figure 2 shows the effects on transmission of increasing the gap width between a single layer of parallel yarns, as a function of the phase change, φ_M, induced in a wave passing through the yarn with effective refractive index, n, and diameter, d.

The maximum attenuation of the transmitted beam occurs at $\varphi_M \sim 4$ and increases rapidly with the yarn gaps. For typical shirt fabric with yarn 0.2 mm diameter, this attenuation peak is around 3 THz. For thicker fabrics with an open weave, the wavelength at which this attenuation peak occurs will be proportional to the yarn diameter. The energy lost from the directly transmitted beam is scattered and diffused in the forward direction. More densely woven fabrics without gaps produce an attenuation steadily rising with frequency over this range.

C. Powders

For powders comprising randomly shaped grains no simple phase distribution function can be written down, but several general conclusions can be drawn from the model. With the slice thickness, d, taken to be equal to the diameter of the largest grains, the maximum phase change is φ_M above [Eq. (6)]. The moments, M_r, of the distribution P are proportional to but cannot exceed φ_M^r. It follows from Eq. (7) that a frequency expansion of the layer transmission is related to the moments of P. In lowest order the mean free path is $d/(M_2 - M_1^2)$with

$$M_r = \int_0^{\varphi_M} P(\varphi)\varphi^r d\varphi. \tag{8}$$

For wavelengths, λ, larger than the particle size, $\varphi_M < 1$, only the low order moments contribute to F. The first moment, M_1, is given by $c\varphi_M$, where c is the volume fraction occupied by the scatterers. The range of possible values of $P(\varphi)$ between zero and φ_M limits the possible values of M_2. This leads to the formula

$$\mathrm{MFP} \sim \lambda^2/dc(1-c)[\pi(n-1)]^2. \tag{9}$$

The numerical factor, of order unity, depends on the range of particle sizes.

D. Spheres

The measurements of Pearce and Mittleman[10] on terahertz transmission through PTFE spheres provide a critical test of any theory of propagation of terahertz waves through random media. The diameter, refractive index, and mean density of the randomly arranged spheres are known. A validation method for the PDM is to calculate the total scattering cross section of an isolated dielectric sphere and compare with the well established results of Mie theory. This shows that, for refractive indices not more than about 1.5, the PDM gives a good qualitative and quantitative match to the exact results. Figure 3 shows that the positions and magnitudes of the scattering peaks and the short wavelength limit are well reproduced. At long wavelengths, where the weak Rayleigh scattering mechanism predominates, the scattering cross section is at least an order of magnitude less than the geometrical cross section and is proportional to the fourth power of frequency. In this region the PDM predicts a cross section proportional to frequency squared, but the absolute error is small. An adjustment factor, described below, allows for this effect.

In calculating the phase change produced by a layer of spheres, a truncated Poisson distribution is used to give the expectation of the number of spheres intersecting a given line of projection through the layer. In order to avoid part spheres, complete spheres with centers inside the layer are included. If the spheres were independent, the number intersected by the line would follow a Poisson distribution, with a mean given by the number density and the layer thickness. The nonoverlapping condition limits the maximum number that can be on one line, and this is approximately allowed for

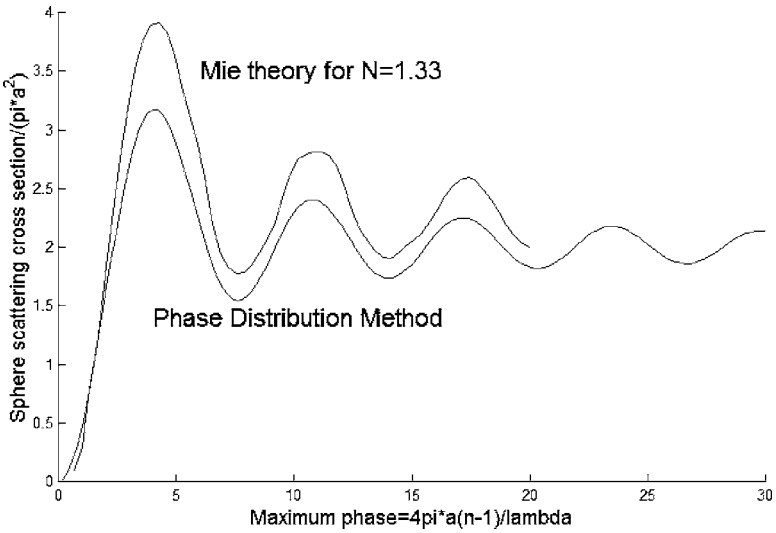

FIG. 3. Total scattering of dielectric sphere showing Mie theory compared with the PDM without the long wavelength correction.

by truncating the Poisson distribution at T proportional to the ratio of layer thickness, d, to sphere diameter, and renormalizing the distribution. If the phase distribution for one sphere is $P_S(\varphi)$ as given in Eq. (3), the amplitude transmission through the layer is given by

$$F = \sum_{r=0}^{T} p_r F_1^r, \tag{10}$$

where p_r is the probability of r spheres being intersected by a given line of projection, and F_1 is given by Eq. (2). The convolution theorem has been used to combine distributions, P_S, assumed to be independent. The mean value M of the probabilities, p_r, is given by the product of the cross section area of the scatterers and the number of scatterers per unit area of the layer. Nonintegral values of the truncation number, T, are allowed for by truncating at integer, s, and including a fraction of the last term in the series for F. This avoids discontinuous changes as the layer thickness is varied. Normalizing the truncated series

$$F = f(T, MF_1)/f(T, M), \tag{11a}$$

with

$$f(T,X) = \sum_{r=0}^{s} \frac{X^r}{r!} + \frac{(T-s)X^T}{\Gamma(T+1)}, \tag{11b}$$

and $s < T < s+1$.

The mean free path follows from Beer's law,

$$|F|^2 = \exp(-d/\mathrm{MFP}). \tag{12}$$

For wavelengths, λ, several times larger than the sphere diameters ($2a$), the amplitude given by Eqs. (2) and (4) requires modification. Comparison of the total scattering cross section for an isolated sphere, index n, calculated by Mie theory, with that from the phase distribution model, suggests that using an effective refractive index for the sphere can allow for Rayleigh scattering,

$$n_{\mathrm{eff}} = 1 + (n-1)/[1 + 0.025(\lambda/a)^2]. \tag{13}$$

Use of this effective index in the phase model matches the exact results for the cross section of an isolated sphere over the whole range of wavelengths (Fig. 3) and we therefore adopt this form in modeling the attenuation for a collection of spheres.

Figure 4 shows the comparison of the calculated MFP with the measurements of Pearce and Mittleman. The overall trend is well modeled, but the subsidiary oscillations of unknown origin are not described. A tentative calculation of the effects of multiple reflections in the sample cell gives similar oscillations, but further experimental details would be needed to confirm this explanation.

III. EXPERIMENTAL ARRANGEMENTS

A. Terahertz frequency measurement system

Terahertz transmission was investigated through random structures with both known and unknown properties to validate theory. The experiments reported here were carried out using a standard terahertz time domain spectrometer (TDS). The terahertz emitter consisted of two chrome-gold electrodes fabricated on low temperature grown gallium arsenide (LT-GaAs), separated by 400 μm and of length 8 mm. An ultrafast Ti-sapphire laser (Coherent Inc.) was used to gener-

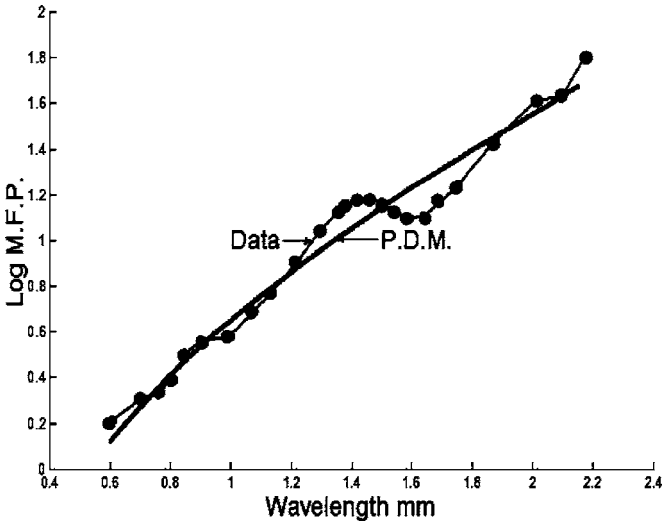

FIG. 4. Mean free path for PTFE spheres, diameter of 0.794 mm.

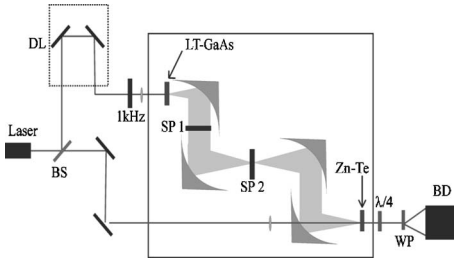

FIG. 5. Terahertz transmission experimental set up (BS=beam splitter, DL=delay line, WP=Wollaston prism, λ/4=quarter wave plate, BD =balanced detector).

ate terahertz pulses. The laser had the following characteristics: bandwidth of 45 nm, pulse lengths of approximately 25–30 fs, 76 MHz repetition rate, and center wavelength of 790 nm. The laser beam was focused onto the edge of one of the electrodes, which were biased at 250 V dc to generate terahertz radiation. After collection and focusing of the terahertz radiation using parabolic mirrors, coherent detection was performed using electro-optic sampling techniques. All parabolic mirrors used were of diameter 5 cm. The collection mirror had focal length 5 cm, the two intermediate mirrors had 10 cm focal lengths, and a mirror of focal length 7.5 cm focused the radiation on to the detector. The probe laser beam, formed by splitting 10% from the pump beam, was incident concurrently with the terahertz pulses onto a 1 mm thick Zn–Te crystal (Ingcrys Ltd). Lock-in detection, using a 1 kHz mechanical chopper placed in the pump arm, was used to measure the electric field of the terahertz pulse. Pulses of bandwidth 3 THz, with peak power at 0.9 THz and signal-to-noise ratio of 7000:1, were routinely obtained with this arrangement. The whole system was enclosed in a dry nitrogen atmosphere. Figure 5 shows a schematic of the experimental setup. It should be noted that the transmission measurements were carried out using both focused (sample position 2) and unfocused beams (sample position 1).

B. Arrays of cylinders

These arrays were used to mimic textile fibers. Although they possessed a random structure, the cylinder radius and the concentration of scatterer material were known. Each phantom consisted of a number of parallel, randomly arranged, cylinders of height 10.0 mm. Within each sample the cylinder diameter was constant, but varied from phantom to phantom in the range of 0.4–1.0 mm. The phantoms also had different concentrations of scattering material with volume fractions ranging from 10%–50% placed on a base of size $20\times x$ mm^2, where $x=1$, 3, or 5. Construction of the arrays proceeded using stereolithographic techniques and an UV curable resin, SI-50, which had a nondispersive refractive index of 1.65 in the terahertz region. Figure 6 shows a plan view of one such sample with cylinder diameter of 0.4 mm and volume fraction of 10%. Focused and unfocused terahertz beams were used to study these arrays. When using the unfocused beam, the phantoms were placed in a metallic holder with surface area greater than the area of the terahertz beam in order to block radiation that would otherwise bypass the sample.

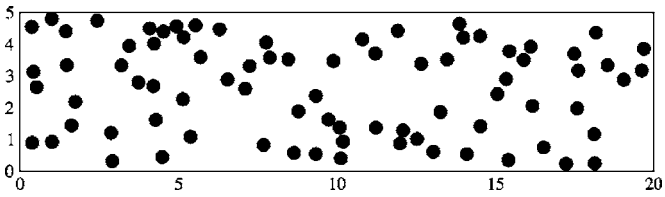

FIG. 6. Plan view of phantom of cylinders, diameters=0.4 mm, volume fraction=10%.

C. Fabrics

Terahertz transmission was investigated through three fabrics of increasingly random internal structure: cotton shirt, tweed, and fleece. The shirt had a very regular warp and weft structure: both yarns were of diameter 180 μm, while the spacings were 250 and 330 μm, respectively. The tweed had a warp-weft structure with yarn diameter approximately 1.10 mm and a spacing of 1.20 mm for both warp and weft. The fleece had no long range fiber structure on the terahertz scale. The main optical density in this fabric arose from the tufts of the fleece, which were assumed to have height of 3.5 mm (see Sec. VI). The effective refractive indices for these materials, calculated from the observed delay of terahertz pulses as they pass through the materials, were 1.25, 1.15, and 1.05 for the shirt, tweed, and fleece, respectively. Again, focused and unfocused terahertz beams were used to investigate the sample transmission.

D. Random powders

It is suspected that the spectra of substances admixed with powders may be affected by scattering and absorption effects of the powder grains. Terahertz transmission through both highly-absorbing and nonabsorbing powders was investigated in an initial attempt to model the propagation of terahertz radiation in such situations. Both absorbing and nonabsorbing powders were investigated. The highly absorbing balls were glass spheres of mean diameters 227 and 462 μm, while the nonabsorbing powder was PTFE powder with grains of mean diameters 100, 55, 12, and 1 μm. A quantity of powder was placed in a piece of milled out PTFE, of internal width 2 or 3 mm and wall thickness approximately 0.5 mm.

IV. COMPARISON OF PHASE DISTRIBUTION MODEL WITH MIE THEORY

If an object of geometrical cross section, S, and total scattering cross section, Q, intercepts a plane wave with area, W, the fraction of the incident power remaining in the unscattered beam, I, is defined by $(1-Q/W)$, and the fraction lost by scattering and absorption is Q/W. The corresponding phase distribution is

$$P(\varphi)=[(W-S)\delta(\varphi)+SP_S(\varphi)]/W, \tag{14}$$

where P_S is the phase distribution projected within the geometrical area of the scatterer. The fractional transmitted intensity, I, is $|F|^2$ and using Eq. (2),

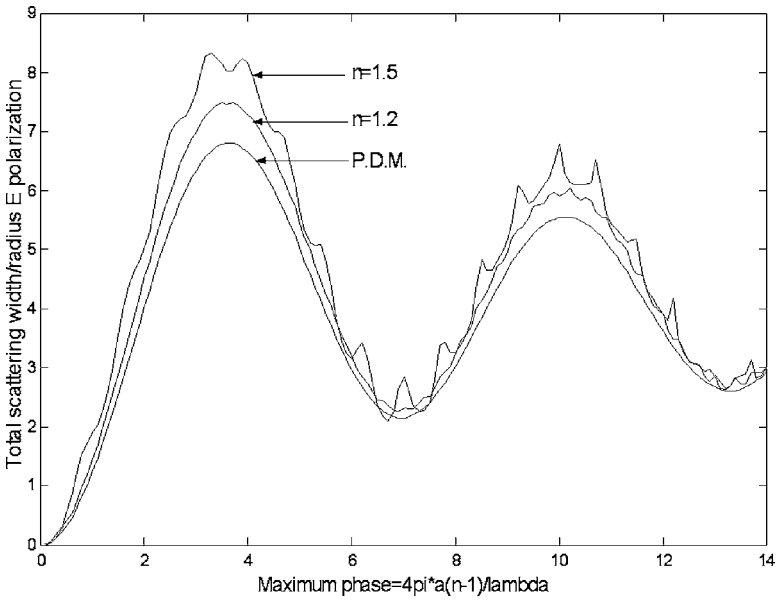

FIG. 7. Total scattering by a dielectric cylinder.

$$I = 1 - \frac{2S}{W}\left[1 - \int P_S(\varphi)\cos\varphi d\varphi\right] + O\left(\frac{S^2}{W^2}\right). \quad (15)$$

At short wavelengths, the distribution, P, will range over many periods, and the cosine integral will approach zero. The cross section then limits to twice the geometrical area. For a meaningful measurement of scattering, the area of the wave front must be much larger than the size of the scatterer, and $(S/W) < 1$. Terms in (S^2/W^2) can then be neglected, and the total scattering cross section is

$$Q = 2S\left[1 - \int P_S(\varphi)\cos\varphi d\varphi\right]. \quad (16)$$

This formula for Q has been compared with exact results for spheres and cylinders. The approximation becomes exact as the refractive index approaches unity and gives excellent agreement for indices less than about 1.5, as shown in Fig. 7. The phase distribution model does not reproduce the surface wave resonances that appear at higher index values.

V. COMPARISON OF PHASE DISTRIBUTION MODEL AND EXPERIMENT: ARRAYS OF CYLINDERS

As discussed earlier, an array of cylinders may be regarded as a useful model to predict the propagation properties of terahertz radiation through garments. It is predicted that, at certain frequencies, high and low terahertz transmissions will occur for a beam propagating through a random array of cylinders. The regions of low transmission arise because of destructive interference between waves propagating through gaps and through cylinders. The only input parameters required for the model are the diameter and volume fraction occupied by the scatterers. These factors determine the number of regions of high and low transmissions and the frequencies at which they occur. Figure 8 shows transmission through a phantom containing 10% scatterers of diameter 0.4 mm, while Fig. 9 shows transmission for a phantom containing 40% scattering material of diameter 1.0 mm. The frequencies of high and low transmissions, as predicted by the model, provide a reasonable description of the experimental data.

VI. COMPARISON OF PHASE DISTRIBUTION MODEL AND EXPERIMENT: TEXTILES

A. Oblique transmission

For a wave incident obliquely onto a layer of fabric, the effects of warp and weft yarn can be considered separately. For a single layer of parallel vertical yarns, the incident beam may be tilted away from normal incidence in either the altitude or azimuthal directions. For beam tilts in altitude, the widths of yarn and gaps projected into the propagation direction are unchanged, but the wave passes obliquely through the yarns, and the optical path and resulting phase change are increased. Figure 2 shows that for frequencies below the at-

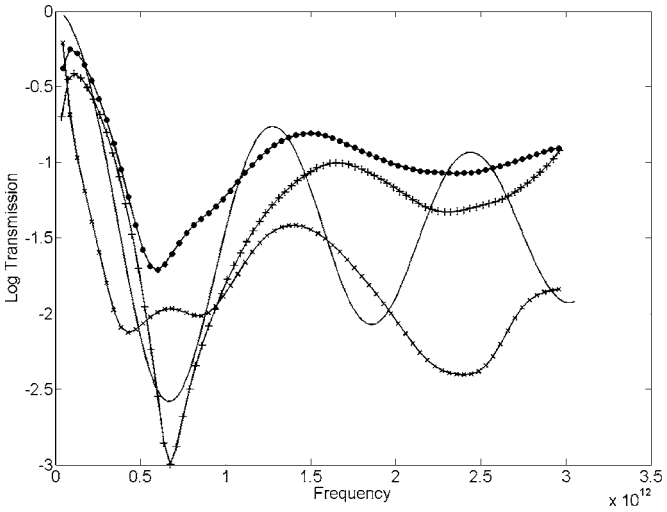

FIG. 8. Transmission through 10% concentrated array with cylinder diameters=0.4 mm [focused beam (squares), unfocused beam, E, perpendicular to cylinders (dots), unfocused beam, E, parallel to cylinders, (crosses), theory (solid)].

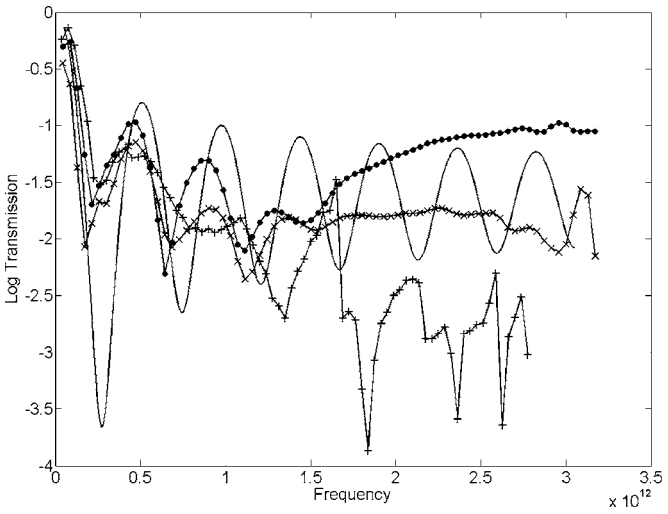

FIG. 9. Transmission through 40% concentrated array with cylinder diameters=1.0 mm [focused beam (squares), unfocused beam, *E*, perpendicular to cylinders (dots), unfocused beam, *E*, parallel to cylinders (crosses), theory (solid)].

tenuation peak, increasing the phase change is equivalent to increasing the frequency and results in increased attenuation.

For beam tilts in azimuth, the path length through the yarns is not increased, but the projected gaps are reduced, and the range of distribution P is narrowed. Figure 2 shows that this reduces the attenuation. For a fabric containing orthogonal warp and weft, an obliquely incident beam will experience a combination of these opposite effects. Numerical calculations for a fabric with identical warp and weft show almost complete cancellation, so that the transmission is independent of angle of tilt up to about 50°. For larger angles, surface reflection becomes increasingly important.

B. Fleece transmission

A fleece consists of randomly arranged tufts supported by a woven fabric. The main contribution to the optical thickness is due to the closely spaced tufts, which have profiles described in the examples in the Appendix. The phase distributions can be summarized by

$$P = \frac{1}{\varphi_S}\left[1 + f\left(\frac{2\varphi}{\varphi_S} - 1\right)\right], \tag{17}$$

where the shape factor, f, lies between −1 and +1 and corresponds to shapes of the tufts from semiellipsoids to cones. The tufts contain a large fraction of trapped air, and have a low terahertz refractive index of order 1.05–1.1, with heights of a few millimeters.

C. Shirts and thin fabrics

For the case of thin fabrics, such as shirts, where the maximum phase changes produced by the yarn are small, it is possible to derive a simple analytical expression for the transmission. The low order moments defined below can be evaluated analytically for cylindrical yarns, giving the intensity transmitted through a set of parallel yarns with diameter, d, and repeat distance, w.

$$I = 1 - \varphi_M^2\left[\frac{2}{3}y - \left(\frac{\pi y}{4}\right)^2\right] + O(\varphi_M^4), \tag{18}$$

with $y=d/w$ and $\varphi_M<1$ [using Eqs. (8) and (10)]. The transmission through the fabric is then a product of separate factors for warp and weft.

D. Tweed

The wool fibers of a typical tweed jacket are of a larger diameter (~0.06 mm) than the fibers of a shirt or fleece. It is no longer valid to treat the yarns as uniform cylinders, as in the shirt example. The simplest model treats the tweed as a random collection of wool fibers, occupying an assumed volume fraction of 0.5, and uses an empirically adjusted wool fiber refractive index (~1.55) to match the experimental data. This results in a steadily rising attenuation to at least 2 THz.

Typical experimental results, with modeling, for a shirt, tweed, and fleece, are shown in Fig. 10. No real difference is seen experimentally when using either the focused or the unfocused beams. These experimental results have been Gaussian smoothed to reduce noise, since fabrics have no sharp spectral features in the terahertz region. The effective indices (see Sec. III) have been empirically adjusted to give the best fit to the data in the absence of definite information at these frequencies.

VII. COMPARISON OF PHASE DISTRIBUTION MODEL AND EXPERIMENT: POWDERS

Figure 11 shows terahertz transmission through PTFE spheres of 100 and 55 μm diameters. The experimental data are compared with the predictions of the PDM. Effective refractive indices and volume fractions were calculated from the pulse delay formula. The 55 μm grain diameter powder had a volume fraction of approximately one-half that of the 100 μm powder. It should be noted that the two smaller diameter powders investigated (not shown in the figure) are more attenuating than the 55 μm powder. This, together with the low volume fraction of the 55 μm powder, indicates that the smaller diameter powders are not evenly dispersed.

Figure 12 shows transmission through both 2 and 3 mm of 227 μm glass balls. These are heavily absorbing; no real transmission is seen at frequencies above approximately 0.6 THz. Similar results are seen for larger diameter balls. Since the transmission is approximately the same through both thicknesses, absorption and dielectric loss effects dominate the scattering process. Any remaining nonabsorbed high frequency photons are completely diffused by scattering within the sample.

VIII. CONCLUSION

The PDM provides a satisfactory overall description of the propagation of terahertz radiation through inhomogeneous materials, which are of considerable interests as "targets" for security and surveillance systems. In such random, unstructured arrays the separation of the scattering centers,

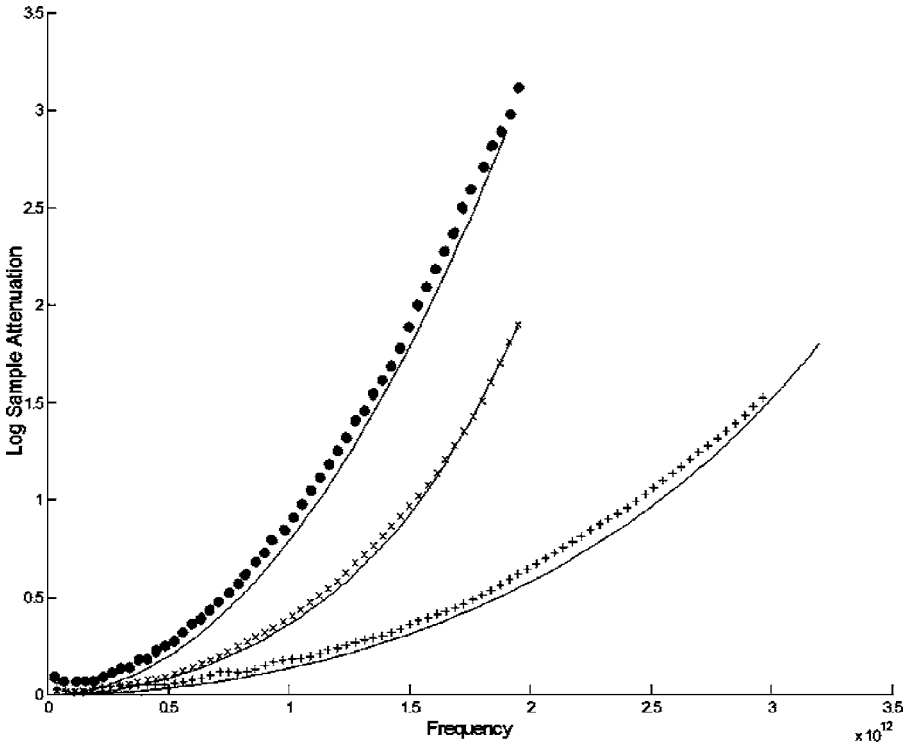

FIG. 10. Attenuation by various fabrics. Experimental data for Harris tweed (dots), fleece (crosses), shirt (squares), theory (solid).

their size, and the wavelength are of similar magnitudes. The PDM is a practical simulation tool for delivering, within a useful time scale, the transmission and other optical properties of such materials. The model considers the amplitude and phase changes imposed on a wave as it emerges from a layer within the scattering material. The properties of real samples are then simulated by taking a sequence of such layers. The predictions of the PDM are compared with those of exact (Mie) theory for isolated scattering centers and with experimental results reported by other workers.[2,3] The PDM is seen to provide a useful description for such cases over the full range of wavelengths. Experimental measurements using a broadband terahertz spectrometer, of the transmission properties of arrays of cylinders (designed to mimic textiles), powders of absorbing and nonabsorbing materials, and of a number of common textiles are presented. For cylinder arrays, regions of low and high transmissions arise due to interference effects. These are reproduced by the simulations, and transmission at high and low frequencies is satisfactorily predicted. For actual textiles, the PDM provides a very good description up to 3 THz. The PDM also describes transmission through nonabsorbing powders very well. In the case of absorbing samples (glass balls) a strong decay in transmission up to approximately 800 GHz is observed experimentally.

It should be emphasized that, in comparison with complete solutions of Maxwell's equations, the present analytical approach can be implemented easily in MATLAB and can deliver predictions essentially instantaneously. This could be of great value for real surveillance systems operating at tera-

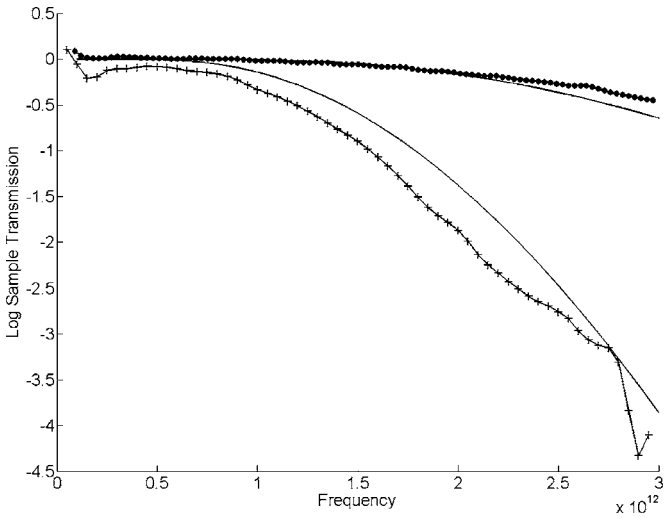

FIG. 11. Comparison of transmission through 100 μm (squares) and 55 μm (dots) PTFE powders with theory (solid).

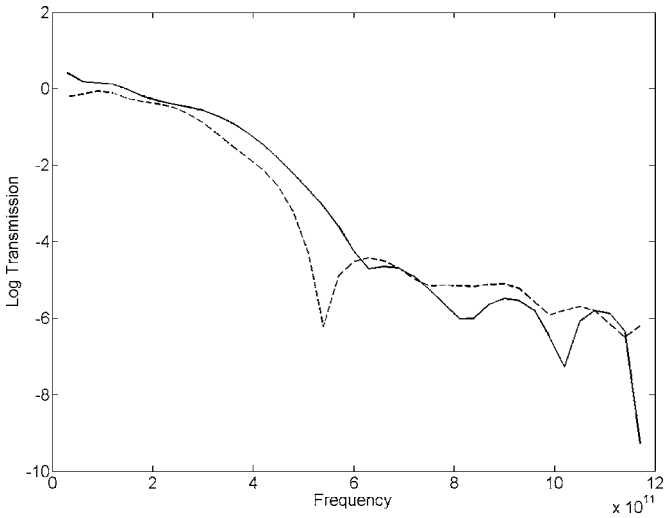

FIG. 12. Transmission through 2 mm (solid) and 3 mm (dashed) of 270 μm diameter glass balls.

hertz frequencies. The PDM and validation measurements are now being extended to include back- and forward-scattering (angular dependent) cases.

ACKNOWLEDGMENTS

The authors wish to acknowledge the support of the Commission of the European Communities for the TeraNova Integrated Project (IST 511415), of which this work forms part. The authors also wish to express thanks to Her Majesty's Government Communications Centre, Qinetiq plc, together with the North East Region Development Agency, and the Engineering and Physical Science Research Council, of the United Kingdom.

APPENDIX

The distribution, P, can be calculated analytically by direct integration for simple shapes such as spheres, cones, or cylinders. For more general shapes, the projected optical thickness of the layer of scattering medium can be evaluated numerically for uniformly distributed positions over a representative area of the layer and the values collected to build the distribution function.

For example, if the scatterer has circular symmetry, φ is dependent on radius, r, within the geometrical cross section area, πa^2, and the phase distribution for the scatterer is

$$P_S(\varphi) = -\frac{d(r^2/a^2)}{d\varphi}, \quad 0 \leqslant \varphi \leqslant \varphi_S, \tag{A1}$$

where φ_S is the maximum phase change produced.

Example (1): Sphere or ellipsoid,

$$\varphi_{\mathrm{sp}}(r) = \varphi_S\sqrt{1-(r/a)^2}, \tag{A2}$$

$$P_{\mathrm{sp}} = 2\varphi/\varphi_S^2. \tag{A3}$$

Example (2): Paraboloid,

$$\varphi_{\mathrm{par}}(r) = \varphi_S[1-(r/a)^2], \tag{A4}$$

$$P_{\mathrm{par}} = 1/\varphi_S. \tag{A5}$$

Example (3): Cone,

$$\varphi_{\mathrm{cone}}(r) = \varphi_S\left(1-\frac{r}{a}\right), \tag{A6}$$

$$P_{\mathrm{cone}} = \frac{2}{\varphi_S}\left(1-\frac{\varphi}{\varphi_S}\right). \tag{A7}$$

[1] D. M. Mittleman, M. Gupta, R. Neelamani, R. G. Baraniuk, J. V. Rudd, and M. Koch, Appl. Phys. B: Lasers Opt. **68**, 1085 (1999).
[2] J. Pearce and D. M. Mittleman, Physica B **338**, 92 (2003).
[3] Z. Jian, J. Pearce, and D. M. Mittleman, Phys. Rev. Lett. **91**, 033903 (2003).
[4] S. Mujumdar, K. J. Chau, and A. Y. Elezzabi, Appl. Phys. Lett. **85**, 6284 (2004).
[5] J. A. Ratcliffe, Rep. Prog. Phys. **19**, 188 (1956).
[6] J. A. Fejer, Proc. R. Soc. London, Ser. A **220**, 455, (1953).
[7] A. Ishimaru, *Wave Propagation and Scattering in Random Media* (Academic, New York, 1978).
[8] M. Born and E. Wolf, *Principles of Optics* (Cambridge University Press, Cambridge, 1999), Chap. 9.
[9] J. E. Bjarnason, T. L. J. Chan, A. W. M. Lee, M. A. Celis, and E. R. Brown, Appl. Phys. Lett. **85**, 519 (2004).
[10] J. Pearce and D. M. Mittleman, Opt. Lett. **26**, 2002 (2001).